On the Number of Water Molecules Necessary To Stabilize the Glycine Zwitterion

Jan H. Jensen and Mark S. Gordon*

Contribution from the Department of Chemistry and Ames Laboratory US-DOE, Iowa State University, Ames, Iowa 50011-3111

Received March 27, 1995[⊗]

Abstract: A thorough *ab initio* study of how the addition of successive water molecules shifts the gas phase zwitterion−neutral equilibrium of the amino acid glycine toward that of the solution phase is presented. Of particular interest is the number of water molecules necessary to stabilize the zwitterion, and how the solvent effects conformational preference. It is found that two water molecules can stabilize the glycine zwitterion, that is, give rise to a potential energy minimum with at least one vibrational level. The results are analyzed and explained using localized charge distributions.

I. Introduction

Elucidating the effect of solvent on structure and reactivity at the molecular level poses a formidable challenge to experiment and theory alike. Much progress has been made in this area,[1] but "a set of unifying principles describing chemical dynamics in liquids"[1b] remains elusive. However, it is generally agreed upon that a clear understanding will involve both solute and solvent dynamics and their coupling, rather than simply solute dynamics under the influence of some representation of the solvent. These molecular solvent effects are not well understood. The zwitterionic−neutral equilibrium of the amino acid glycine, $^{+}NH_3CH_2COO^{-} \rightleftharpoons NH_2CH_2COOH$ provides a good test case for the study of such effects since it shifts markedly in favor of the zwitterionic form upon aqueous solvation.

As discussed in Section IIIA, the gas phase structure of glycine is fairly well understood. The zwitterionic form of glycine does not appear to exist in the gas phase.[2−4] The neutral potential energy surface (PES) of glycine has been studied both theoretically[5] and experimentally.[6]

At room temperature the bulk aqueous form of glycine is predominantly zwitterionic for pH = 2−10 (ref 7) with the zwitterionic form favored by a free energy and enthalpy of 7.2 and 10.3 kcal/mol,[8] respectively. Various NMR relaxation techniques have been used to study the kinetics of intramolecular proton transfer[9] in aqueous solution and all yielded a free energy of activation of about 14.3 kcal/mol for proton transfer. One study[9c] determined the rate constant at several temperatures and derived enthalpy and $-T\Delta S$ contributions to the free energy of activation of −0.2 and 14.6 kcal/mol, respectively! It should be noted that the NMR studies are unable to distinguish between intramolecular and water-catalyzed proton transfer mechanisms and this can complicate the thermodynamic interpretation of the rate constant if both are important. Other experimental data[10] include a heat of solvation of −19.2 kcal/mol, calculated as the difference in the heat of solution and sublimation of solid glycine.

If the gas phase structure of glycine is defined as a "reactant" and the aqueous structure as a "product", a "reaction path" can be traced by adding successive water molecules to the reactant until the product is reached. Key points along this reaction path are (1) the point at which the zwitterion form becomes a local minimum and (2) the point at which the neutral and zwitterion forms become isoenergetic, as illustrated in Scheme 1. The research described in this paper concerns itself with the first point. Important questions to be answered in this regard are as follows: (1) Why is there no barrier to proton transfer in the gas phase? (2) How does the solvent induce a barrier and thus stabilize the zwitterion? (3) Can the solvent participate directly in the proton transfer, and if so, how does this mechanism differ from the gas phase mechanism?

Several theoretical studies on the solvation of glycine have been published. Bonaccorsi et al.[11] used a continuum reaction field method and obtained a zwitterionic−neutral free energy difference of 5.6 kcal/mol and a heat of solvation of −19.5 kcal/mol; in both cases the 4-31G basis set was employed. Rzepa and Yi[12] combined the continuum and supermolecule approach in a semiempirical study on glycine−water clusters. The remaining, discrete solvation studies on glycine can be divided

[⊗] Abstract published in *Advance ACS Abstracts*, July 15, 1995.

(1) (a) Fleming, G. R.; Wolynes, P. G. *Phys. Today* **1990**, *43*, 36. (b) Rossky, P. J.; Simon, J. D. *Nature* **1994**, *370*, 263.

(2) Ding, Y.; Krogh-Jespersen, K. *Chem. Phys. Lett.* **1992**, *199*, 261.

(3) (a) Tse, Y.-C.; Newton, M. D.; Visheshwara, S.; Pople, J. A. *J. Am. Chem. Soc.* **1978**, *100*, 4329. (b) Yu, D.; Armstrong, D. A.; Rauk, A. *Can. J. Chem.* **1992**, *70*, 1762.

(4) Langlet, J.; Caillet, J.; Evleth, E.; Kassab, E. *Modeling of Molecular Structure and Properties*; Proceedings of an International Meeting, Nancy, France. Revail, J.-E., Ed. *Studies in Physical and Theory Chemistry*; Elsevier: Amsterdam, 1990; Vol. 71.

(5) (a) Ramek, M.; Cheng, V. K. W.; Frey, R. F.; Newton, S. Q.; Schäfer, L. *J. Mol. Struct.* **1991**, *245*, 1. (b) Jensen, J. H.; Gordon, M. S. *J. Am. Chem. Soc.* **1991**, *113*, 3917. (c) Császár, A. G. *J. Am. Chem. Soc.* **1992**, *114*, 9568. (d) Hu, C.-H.; Schaefer, H. F., III. *J. Am. Chem. Soc.* **1993**, *14*, 1347. (e) Barone, V.; Adamo, C.; Lejl, F. *J. Chem. Phys.* **1995**, *102*, 364.

(6) (a) Brown, R. D.; Godfrey, P. D.; Storey, J. W. V.; Bassez, M. P. *J. Chem. Soc., Chem. Commun.* **1978**, 547. (b) Suenram, R. D.; Lovas, F. J. *J. Mol. Spectrosc.* **1978**, *72*, 372. (c) Suenram, R. D.; Lovas, F. J. *J. Am. Chem. Soc.* **1980**, *102*, 7180. (d) Iijima, K.; Tanaka, K.; Onuma, S. *J. Mol. Struct.* **1991**, *246*, 257. (e) Godfrey, P. D.; Brown, R. D. *J. Am. Chem. Soc.* **1985**, *117*, 2019.

(7) Maskill, H. *The Physical Basis of Organic Chemistry*; Oxford University Press: Oxford, UK, 1985; p 162.

(8) Wada, G.; Tamura, E.; Okina, M.; Nakamura, M. *Bull. Chem. Soc. Jpn.* **1992**, *55*, 3064.

(9) (a) Sheinblatt, N.; Gutowsky, S. *J. Am. Chem. Soc.* **1964**, *86*, 4814. (b) Chang, K. C.; Grunwald, E. *J. Phys. Chem.* **1976**, *80*, 1422. (c) Slifkin, M. A.; Ali, S. M. *J. Mol. Liq.* **1984**, *28*, 215.

(10) Gaffney, J. S.; Pierce, R. C.; Friedman, L. *J. Am. Chem. Soc.* **1977**, *99*, 4293.

(11) Bonaccorsi, R.; Palla, P.; Tomasi, J. *J. Am. Chem. Soc.* **1984**, *106*, 1945.

(12) Rzepa, H. S.; Yi, M. Y. *J. Chem. Soc., Perkin Trans. 2* **1991**, 531.

0002-7863/95/1517-8159$09.00/0

Scheme 1. "Reaction Path" Leading from the Glycine Zwitterion–Neutral Equilibrium in the Gas Phase to That in Bulk Aqueous Solution

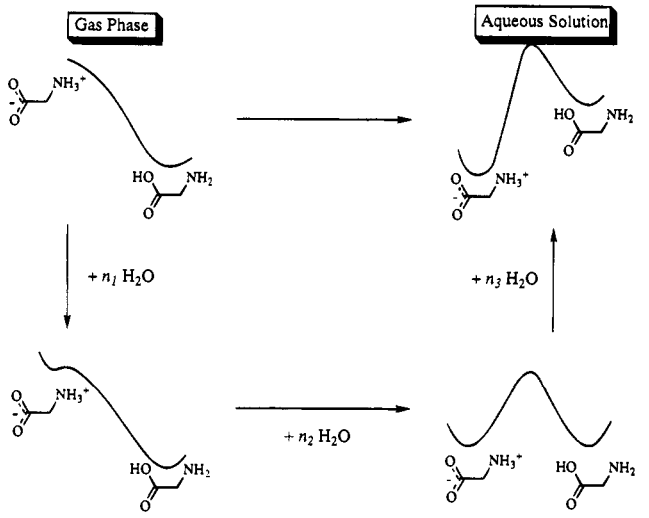

into two groups. One is Monte Carlo studies employing classical potentials and a large number of water molecules.[13] The other is quantum mechanical studies on relatively small glycine–water clusters.[4,14,15] The two studies that are particularly relevant to this study report SCF calculations, using split valence basis sets, on one water molecule complexed with zwitterionic[4] and neutral[15] glycine and will be discussed in the appropriate sections of this paper.

II. Computational Methodology

1. Geometries. Molecular geometries were calculated at the restricted Hartree–Fock (RHF) level of theory using Dunning's DZP[16] [DZ(d,p)] basis set. For reasons explained later, geometries on the PES of gas phase glycine were calculated at the RHF/6-31G(d)[17] (6-31G*) level of theory. Some other preliminary geometry optimizations were also performed at this level of theory. The nature of all stationary points was verified by calculating the eigenvalues of the matrix of energy second derivatives (Hessian). Stationary points with n negative eigenvalues can follow n downhill directions that lead to lower energy structures, so that minima and transition states have 0 and 1 negative eigenvalues, respectively. Upon conversion to frequencies, the unscaled[18] eigenvalues are used to calculate zero point vibrational energies and free energies at 298 K using the harmonic oscillator–rigid rotor approximation.

2. IRCs. The nature of all RHF/DZP transition states was verified by tracing the intrinsic reaction coordinate (IRC) from the transition state to the two lower energy structures it connects by using the second-order Gonzales–Schlegel integration method.[19] An IRC is defined as the minimum energy path from the transition state to the reactants and products, traced in mass-weighted Cartesian coordinates. It is typically depicted as a plot of the total energy vs "s", the root mean square displacement of *all* atoms from the previous integration point. Thus, this reaction coordinate contains solute as well as solvent coordinates.

3. Energies and Convergence. The relative energies of most stationary points were evaluated at the MP2/DZP++//RHF/DZP level of theory, where A//B denotes an energy calculation at the "A" level of theory evaluated at the "B" geometries. MP2 denotes second-order Møller–Plesset perturbation theory,[20] and DZP++ denotes the DZP basis set augmented by diffuse s and sp functions on hydrogens and heavier elements, respectively.[21] Two additional sets of MP2 calculations were performed on the glycine(H_2O) system (to be described in detail in Section IIIC) to test how well the DZP++ basis set is converged. The glycine(H_2O) system was chosen over the gas phase glycine system since it also contains intermolecular hydrogen bonds. One MP2 set employs the TZP++[22] basis set to test the importance of triple ζ valence basis sets. The other MP2 set employs the aug-cc-pDZV[23] basis set, which includes diffuse s and p functions on the hydrogen atoms and diffuse s, p, and d functions on the heavier atoms. This basis set has been shown to give essentially converged results for the water dimer.[24] Additionally, a set of MP4[25]/DZP++ calculations were performed to monitor the convergence of the perturbation expansion. Table 1 lists the results. As can be seen, the MP2/DZP++ energy of both the transition state and the neutral structure, relative to the zwitterion, is within 0.6 kcal/mol of the higher level results.

4. Energy Decomposition. The theory of localized charge distributions[26] is used to analyze the total energy and is summarized here. A localized charge distribution (LCD) consists of a localized molecular orbital (LMO, ψ_i) plus its assigned local nuclear charge distribution [Z_i(A) for all atoms A]. A charge distribution of a neutral molecule consisting of $2N$ electrons in N orbitals can be partitioned into N neutral LCDs by setting

$$\begin{aligned} Z_i(A) = 2 \text{ if } \psi_i \text{ is an inner-shell or a lone-pair LMO} \\ \text{predominantly localized on atom A} \\ = 1 \text{ if } \psi_i \text{ is a bond LMO predominantly localized} \\ \text{on atom A and its bonded partner} \\ = 0 \text{ otherwise} \end{aligned} \quad (1)$$

The total nuclear charge on a given atom (A) must be preserved,

$$\sum_{i=1}^{N} Z_i(A) = Z_A \quad (2)$$

where Z_A is the nuclear charge on atom A. Consider the BH molecule as an example. Localizing the electronic wave function yields three

(13) (a) Romano, S.; Clementi, E. *Int. J. Quantum Chem.* **1978**, *14*, 839. (b) David, C. W. *Chem. Phys. Lett.* **1981**, *78*, 337. (c) Mezei, M.; Mehrotra, P. K.; Beveridge, D. L. *J. Biomol. Struct.: Dyn.* **1984**, *2*, 1. (d) Stamato, F. M. L. G.; Goodfellow, J. M. *Int. J. Quantum Chem.: Quantum Biol. Symp.* **1986**, *13*, 277. (e) Alagona, G.; Ghio, C.; Kollman, P. A. *J. Mol. Struct. (Theochem)* **1988**, *166*, 385. (f) Alagona, G.; Ghio, C. *J. Mol. Liq.* **1990**, *47*, 139.

(14) (a) Förner, W.; Otto, P.; Bernhardt, J.; Ladik, J. J. *Theor. Chim. Acta* **1981**, *60*, 269. (b) Kokpol, S. U.; Dungdee, P. B.; Hannongbua, S. V.; Rode, B. M.; Limtrakul, J. P. *J. Chem. Soc., Faraday Trans. 2* **1988**, *84*, 1789 and references therein.

(15) Basch, H.; Stevens, W. J. *Chem. Phys. Lett.* **1990**, *169*, 275.

(16) Dunning, T. H., Jr.; Hay, P. J. *Methods of Electronic Structure Theory*; Schaefer, H. F., III, Ed.; Plenum Press: New York, 1977; Chapter 1.

(17) (a) Hehre, W. J.; Ditchfield, R.; Pople, J. A. *J. Chem. Phys.* **1978**, *14*, 91. (b) Hariharan, P. C.; Pople, J. A. *Theor. Chim. Acta* **1973**, *28*, 213.

(18) The frequencies were not scaled because it is not clear what scale factors to use for the low-frequency librational modes associated with hydrogen bonds.

(19) (a) Gonzales, C.; Schlegel, H. B. *J. Phys. Chem.* **1990**, *94*, 5523. (b) Gonzales, C.; Schlegel, H. B. *J. Chem. Phys.* **1991**, *95*, 5853.

(20) (a) Møller, C.; Plesset, M. S. *Phys. Rev.* **1934**, *46*, 618. (b) Pople, J. A.; Binkley, J. S.; Seeger, R. *Int. J. Quantum Chem.: Quantum Chem. Symp.* **1976**, *10*, 1.

(21) (a) Diffuse sp and s functions were added to non-hydrogen and hydrogen atoms, respectively. The exponents are C 0.0438, N 0.0639, O 0.0845, H 0.0360. (b) Clark, T.; Chandrasekhar, J.; Spitznagel, G. W.; Schleyer, P. v. R. *J. Comp. Chem.* **1983**, *4*, 294.

(22) Dunning, T. H., Jr. *J. Chem. Phys.* **1971**, *55*, 716.

(23) (a) Dunning, T. H., Jr. *J. Chem. Phys.* **1989**, *90*, 1007. (b) Kendall, R. A.; Dunning, T. H., Jr.; Harrison, R. J. *J. Chem. Phys.* **1992**, *96*, 6796. (c) Each d polarization function is described by six Cartesian components rather than the five spherically averaged components used by Dunning et al.

(24) Feller, D. *J. Chem. Phys.* **1992**, *96*, 6104.

(25) Krishnan, R.; Frisch, M. J.; Pople, J. A. *J. Chem. Phys.* **1980**, *72*, 4244.

(26) (a) England, W.; Gordon, M. S. *J. Am. Chem. Soc.* **1971**, *93*, 4649. (b) England, W.; Gordon, M. S. *J. Am. Chem. Soc.* **1972**, *94*, 4818. (c) Gordon, M. S.; England, W. *J. Am. Chem. Soc.* **1972**, *94*, 5168. (d) Gordon, M. S.; England, W. *Chem. Phys. Lett.* **1972**, *15*, 59. (e) Gordon, M. S.; England, W. *J. Am. Chem. Soc.* **1973**, *95*, 1753. (f) Gordon, M. S. *J. Mol. Struct.* **1974**, *23*, 399. (g) England, W.; Gordon, M. S.; Ruedenberg, K. *Theory Chim. Acta* **1975**, *37*, 177. (h) Jensen, J. H.; Gordon, M. S. *J. Phys. Chem.* **1995**, *99*, 8091.

Table 1. Energies (in kcal/mol) of **TS1a** and **N1a** Relative to **Z1a** at Various Levels of Theory[a]

	TS-Z	N-Z
MP2/DZP++	−1.9	−11.8
MP2/TZP++	−1.6	−12.4
MP2/aug-cc-pDZV	−2.0	−11.7
MP4/DZP++	−1.3	−12.2

[a] See section IIIA for the definitions of the nomenclature.

doubly occupied LMOs: an inner-shell, a lone pair, and a bond orbital. The first two are predominantly localized on one atom (B), whereas the bond orbital is localized on both atoms (B and H). These three orbitals can now be used to define their corresponding localized nuclear charge distributions: inner-shell and lone-pair LMOs are assigned +2 charges positioned at the *one* atom on which they are localized, whereas the bond LMOs are assigned +1 charges on each of the *two* atoms on which they are localized:

These three types of localized charge distributions can be used to describe most, but not all, charge distributions. A charge distribution with a formal net charge, for example, requires special attention and is addressed in later sections.

Once the $\{Z_i(A)\}$ are defined, it is possible to partition any molecular expectation value of interest into localized contributions. Of prime interest, of course, is the total molecular SCF energy, E^{SCF}. For a system of N localized orbitals,

$$E^{SCF} = \sum_{i=1}^{N}[T_i + \sum_{j=1}^{N} v_{ij}] \tag{3}$$

The first term is the kinetic energy of the electrons in LMO i. The second term contains the internal potential energy of LCD i plus the interaction potential energy between LCD i and all other LCDs.[26] The MP2 energy correction $[E^{(2)}]$ to the RHF energy can be written as the sum of pair correlation energies of doubly occupied spatial orbitals,

$$E^{(2)} = \sum_{i=1}^{N}\sum_{j=1}^{N} e_{ij}^{(2)} \tag{4}$$

where each $e_{ij}^{(2)}$ is the correlation energy associated with a pair of electrons in LMO i and j.[26h,27] The total energy ($E^{SCF} + E^{(2)}$) can thus be written as

$$E = \sum_{i=1}^{N}[T_i + \sum_{j=1}^{N} v_{ij} + \sum_{j=1}^{N} e_{ij}^{(2)}] \tag{5}$$

5. Calculational Details. Most calculations were performed with the quantum chemistry code GAMESS.[28] Many of the calculations were performed in parallel on a 16 node iPSC/860 Paragon and a local workstation cluster. Some of the MP2 and analytic Hessian calculations were performed with the HONDO program.[29] The MP2 calculations were performed using GAUSSIAN92.[30]

The LMOs used in the LCD analyses were obtained by using the energy localization scheme due to Edmiston and Ruedenberg.[31] This algorithm yields localized molecular orbitals by minimizing interorbital repulsions.

III. Results

A. Nomenclature and Overview. Structures are named as follows. Zwitterionic, transition state, and neutral structures are designated by **Z**, **TS**, and **N**, respectively. These labels are followed by the number **0**, **1**, or **2** indicating the number of water molecules that are associated with the glycine molecule. If necessary, the structures are distinguished from each other by appending the letters **a**, **b**, etc., as they are introduced. For example, structure **Z2b** is the second dihydrated zwitterionic structure discussed in this paper.

Relative classical energies, enthalpies at 0 K, and Gibbs free energies at 298 K are denoted by ΔE, ΔH_0, and ΔG_{298}, respectively. The classical binding energy of a glycine$(H_2O)_n$ complex is defined as:

$$\Delta E_b = E[\text{Gly\#}] + nE[H_2O] - E[\text{complex}] \tag{6}$$

where E[Gly#] is the energy of an isolated glycine molecule whose geometry is fixed at that of the glycine$(H_2O)_n$ complex. We term this distortion energy the "intrinsic glycine energy". $E[H_2O]$ is the energy of a water molecule whose structure has been optimized, which is a constant. The *change* in the binding energy,

$$\Delta\Delta E_b = \Delta E[\text{Gly\#}] - \Delta E \tag{7}$$

can be used, together with the change in the intrinsic energy, to express the change in the total energy,

$$\Delta E = \Delta E[\text{Gly\#}] - \Delta\Delta E_b \tag{8}$$

The relative intrinsic energy provides information about how the glycine geometry is distorted by the solvent.

Key geometric parameters (calculated using RHF/6-31G* for gas phase structures and RHF/DZP for solvated structures) of the structures involved in proton transfer on the gas phase, monohydrated, and dihydrated glycine potential energy are displayed in Figures 1, 3, and 5, respectively. Table 2 lists additional structural information, and Table 3 lists the associated relative energies, and energy components, of these stationary points, based on MP2/DZP++ single point calculations. The associated IRCs are shown in Figure 2. Additional mono- and dihydrated neutral structures and energetics are presented in Figures 4 and 6 and Table 4, respectively. The key finding, to be discussed in detail in the following sections, is that the zwitterion is not a minimum on the glycine$(H_2O)_n$ potential energy surface until $n = 2$.

B. Gas Phase Glycine. 1. Zwitterion PES. As mentioned in the Introduction, the zwitterionic form of glycine does not exist in the gas phase. However, calculations on the isolated zwitterion provide valuable information about the intrinsic chemistry of this species that is necessary for a direct evaluation of solvent effects. Such calculations are possible since some

(27) Petersson, G. A.; Al-Laham, M. A. *J. Chem. Phys.* **1991**, *94*, 6081.
(28) Schmidt, M. W.; Baldridge, K. K.; Boatz, J. A.; Elbert, S. T.; Gordon, M. S.; Jensen, J. H.; Koseki, S.; Matsunaga, N.; Nguyen, K. A.; Su, S.; Windus, T. L.; Dupuis, M.; Montgomery, J. A., Jr. *J. Comp. Chem.* **1993**, *14*, 1347.
(29) (a) Dupuis, M.; Farazdel, A.; Karna, S. P.; Maluendes, S. A. *Modern Techniques in Computational Chemistry*; Clementi, E., Ed.; Escom: Leiden, The Netherlands, 1990; p 277. (b) Dupuis, M.; Chin, S.; Marquez, A. *Relativistic and Electron Correlation Effects in Molecules and Solids*; Malli, G. L., Ed.; Plenum Press: New York, 1994; p 315.
(30) Gaussian 92, Revision A, Frisch, M. J.; Trucks, G. W.; Head-Gordon, M.; Gill, P. M. W.; Wong, M. W.; Foresman, J. B.; Johnson, B. G.; Schlegel, H. B.; Robb, M. A.; Replogle, E. S.; Gomperts, R.; Andres, J. L.; Raghavachari, K.; Binkley, J. S.; Gonzalez, C.; Martin, R. L.; Fox, D. J.; Defrees, D. J.; Baker, J.; Stewart, J. J. P.; Pople, J. A.; Gaussian, Inc.: Pittsburgh, PA, 1992.
(31) (a) Edmiston, C.; Ruedenberg, K. *Rev. Mod. Phys.* **1963**, *35*, 457. (b) Raffenetti, R. C.; Ruedenberg, K.; Janssen, C. L.; Schaefer,. F., III. *Theor. Chim. Acta* **1993**, *86*, 149.

basis sets, notably ones without p-type polarization functions on the hydrogens, predict a shallow minimum on the zwitterionic PES.

A careful study of the RHF/6-31+G* conformational zwitterion PES by Ding and Krogh-Jespersen[2] suggests that there is only one minimum on this surface. The RHF/6-31G* C_s optimized structure of this minimum (**Z0**) is shown in Figure 1a. (A RHF/DZP geometry optimization starting from this geometry resulted in proton transfer to give a neutral structure.) The most important feature of **Z0** is an unusually short intramolecular hydrogen bond distance of 1.55 Å, with an associated NH bond that is 0.071 Å longer than the two other NH bonds. The CO bond *cis* to the NH_3 group is significantly (0.045 Å) longer than the *trans* CO bond, indicating more single bond character for the former bond (Table 2). This is presumably due to the accumulation of negative charge on the *cis* oxygen due to the neighboring positive NH_3 group and its participation in the intramolecular hydrogen bond.

2. Proton Transfer Transition State. The RHF/6-31G* transition state for intramolecular proton transfer is shown in Figure 1b. The structure is very similar to **Z0**: the breaking NH bond is lengthened by a mere 0.027 Å while the H···O distance has shortened by 0.077 Å. The barrier at this level of theory is minuscule (0.02 kcal/mol), and disappears when vibrational effects and electron correlation (MP2/DZP++) are added (Table 3). Figure 2a shows a plot of MP2/DZP++ energies along the RHF/6-31G* IRC. Clearly, at this level of theory the zwitterionic minimum does not exist.

3. Neutral PES. The IRC in Figure 2a leads to the neutral structure **N0a** shown in Figure 1c. This structure also has an intramolecular hydrogen bond, albeit much weaker than in **Z0** based on the hydrogen bonding distance of 1.97 Å. The proton transfer reaction in Figure 1 is exothermic by 17.0 kcal/mol on the classical potential energy surface. Addition of vibrational zero point corrections (to give ΔH_0) and of entropy effects (to give ΔG_{298}) raises this number to −16.4 and −16.0 kcal/mol, respectively (see Table 3). The neutral PES of gas phase glycine has been studied extensively and it is known[5] that **N0b**,

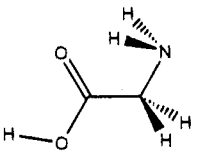

N0b (C_s)

and not **N0a**, is the global minimum. At the RHF/6-31G* level of theory **N0a** is a transition state connecting two isoenergetic C_1 minima on the electronic PES. However, the first vibrational level in this double well is higher in energy than the barrier connecting the two wells, and **N0a** appears to be a minimum on the H_0 surface.[5b] At the MP2/DZP++//RHF/6-31G* level of theory, **N0a** is 1.0 kcal/mol higher in energy than **N0b**. Adding H_0 or G_{298} energy corrections increases this number to 1.1 and 1.8 kcal/mol, respectively, as shown in Table 3. Thus the overall exothermicity of the **Z** → **N** proton transfer reaction in the gas phase is 18.0 kcal/mol on the classical potential energy surface.

C. Glycine(H_2O). 1. Zwitterion PES. The monohydrated zwitterion surface was initially explored at the RHF/6-31G* level of theory to select candidates for geometry optimizations at the RHF/DZP level of theory. Since both glycine and water have planes of symmetry, C_s structures are possible. Thirteen C_s stationary points were considered first, and these are shown in Scheme 2. Of these C_s structures, three have the water hydrogen bonded to the COO^- group (**i**−**iii**), four to the NH_3^+ group (**v**−**viii**), and six to both groups (**ix**−**xiv**). Structures **iii** and **x** had been located previously by Langlet et al.[4]

Table 2. Selected Structural Parameters for the Stationary Points Discussed in This Paper[a]

	$r(CO_{cis})$	$r(CO_{trans})$	ϕ
Z0	1.248	1.203	0.0
TS0	1.253	1.200	0.0
N0a	1.316	1.185	0.0
Z1a	1.249	1.209	−0.5
Z1b	1.236	1.222	−36.5
TS1a	1.271	1.200	−3.4
TS1b	1.271	1.200	28.7
N1a	1.320	1.191	−27.0
N1b	1.318	1.189	44.4
Z2a	1.252	1.211	−16.0
Z2b	1.254	1.208	0.0
Z2c	1.229	1.229	−103.0
TS2a	1.277	1.200	−7.0
TS2b	1.284	1.200	−32.7
TS2c	1.271	1.208	−58.4
N2a	1.317	1.195	−20.6
N2b	1.313	1.195	−65.8
N2c	1.315	1.195	−67.9

[a] O_{cis} refers to the glycine oxygen atoms involved in the proton transfer, and ϕ is the dihedral angle, N−CC−O_{cis}. Distances are in Å and angles are in degrees. See section IIIA for the definitions of the nomenclature.

Structure **i** appears to be the only C_s minimum on the RHF/6-31G* zwitterion PES. A RHF/DZP geometry optimization initiated from this RHF/6-31G* geometry (and hessian) leads to a neutral structure, so **i** does not appear to be a minimum on the RHF/DZP zwitterion PES. Structure **ii** has one imaginary frequency with an a″ normal mode corresponding to rotation about the C−N bond and is a transition state for NH_3^+ rotation in **i**. Structure **iii** has a very small ($14i$ cm^{-1}) imaginary frequency. Following the a″ mode associated with this frequency led to the C_1 structure **iv** which is a minimum on the RHF/6-31G* PES but only very slightly lower in energy. However, a search for the corresponding RHD/DZP minimum, using the same procedure as for *i*, led to a neutral structure.

All the remaining structures, **v**−**xiv**, have 1−3 imaginary frequencies with associated a″ modes. Structures with water hydrogens out of the plane of symmetry are invariably higher in energy than structures with in-plane water hydrogens for a given water−zwitterion arrangement. The former structures invariably have an imaginary frequency with a mode that is predominantly water rotation—a motion that leads to the latter, lower energy, structures. All other distortions, to C_1 geometries, lead to the 6-31G* equivalent of structure **Z1a** shown in Figure 3a upon optimization of the geometry. Additional geometry searches led to structure **Z1b**, shown in Figure 3b. Equivalent structures, verified as minima, are also found on the RHF/DZP PES.

The two zwitterionic minima found on the RHF/DZP monohydrated glycine surface (Figure 3) both have the water molecule bridging the COO^- and NH_3^+ groups. The two structures differ mainly in which oxygen of the COO^- group the water molecule is hydrogen bonded to: for **Z1a** it is the oxygen *cis* to the nitrogen while for **Z1b** it is the *trans* oxygen. The binding energies (eq 6) for **Z1a** and **Z1b** are essentially identical (18.3 and 18.4 kcal/mol, respectively; see Table 4). Both structures **Z1a** and **Z1b** retain the intramolecular hydrogen bond found in the glycine molecule, though the hydrogen bond length in **Z1a** (**Z1b**) is longer by 0.41 Å (0.37 Å) relative to **Z0**. The water−glycine hydrogen bond arrangement introduces only a 0.5° deviation from planarity in the heavy-atom framework of glycine for **Z1a** but a 36.5° deviation for **Z1b** (Table 2). Since

Table 3. MP2/DZP++//RHF/DZP Energies (in kcal/mol) for Proton Transfer Transition States and Resulting Neutral Structures, Relative to the Zwitterion, for Glycine$(H_2O)_n$, $n = 0-2$[a]

	transition state					neutral				
reaction	$-\Delta\Delta E_b$	ΔE[Gly#]	ΔE	ΔH_{ii}	ΔG_{298}	$-\Delta\Delta E_b$	ΔE[Gly#]	ΔE	ΔH_{ii}	ΔG_{298}
Z0 → N0a			−1.0[b]	−1.9[b]	−1.7[b]			−17.0[b]	−16.4[b]	−16.0[b]
Z1a → N1a	5.4	−7.3	−1.9	−4.8	−4.7	10.0	−21.7	−11.8	−12.8	−13.9
Z1a → N1b			3.6	−1.0	0.2	6.7	−17.1	−10.4	−11.1	−11.6
Z2a → N2a	6.4	−7.0	−0.6	−3.6	−3.6	13.1	−20.7	−7.6	−8.4	−8.9
Z2b → N2b	4.7[c]	1.7[d]	6.3	1.3	1.9	8.5[c]	−12.3[d]	−3.8	−5.0	−6.1
Z2c → N2c	5.6[c]	−1.3[d]	4.4	−0.7	0.5	10.8[c]	−16.3[d]	−5.5	−6.7	−7.3

[a] See section IIIA for the definitions of the various terms. [b] These values are calculated at the MP2/DZP++//RHF/6-31G* level of theory. [c] Change in the binding energy of the "spectator" water molecule. [d] Relative intrinsic energy of the glycine(H_2O) system, where the water molecule in assisting the proton transfer.

Table 4. MP2/DZP++//RHF/DZP Binding Energies, Relative Binding Energies, Intrinsic Glycine Energies, and Relative Total Energies of Zwitterionic and Neutral Minima[a]

	ΔE_b	$-\Delta\Delta E_b$	ΔE[Gly#]	ΔE	ΔH_{ii}	ΔG_{298}
N0b				0.0[b]	0.0[b]	0.0[b]
N0a				1.0[b]	1.1[b]	1.8[b]
Z1a	18.3	0.0	0.0	0.0	0.0	0.0
Z1b	18.4	−0.1	1.4	1.3	1.5	1.7
N1c	10.9	0.0	0.0	0.0	0.0	0.0
N1d	11.3	−0.4	1.6	1.2	1.2	1.2
N1e	9.2	1.7	1.7	3.4	3.3	3.3
N1f	7.4	3.5	0.2	3.7	3.3	2.7
N1a	8.3	2.6	1.1	3.7	3.8	3.1
N1g	6.3	4.6	0.9	5.4	5.1	3.8
N1b	11.7	−0.8	5.8	5.6	5.8	5.9
Z2a	34.8	0.0	0.0	0.0	0.0	0.0
Z2b	39.1	−4.3	5.0	0.7	0.9	1.6
Z2c	44.4	−9.6	10.9	1.3	1.9	2.4
N2d	24.4	0.0	0.0	0.0	0.0	0.0
N2e	25.1	−0.7	1.7	1.0	1.0	0.7
N2a	21.7	2.7	0.6	3.3	3.3	2.9
N2f	20.4	4.0	1.3	5.3	4.8	3.7
N2g	18.1	6.3	−0.3	6.0	5.1	3.9
N2c	24.1	0.3	6.4	6.7	6.9	7.0
N2h	18.8	5.6	1.4	6.9	6.5	5.5
N2b	23.2	1.2	6.6	7.8	7.7	7.4
N2i	15.1	9.3	0.4	9.7	9.1	6.4

[a] See section IIIA for the definitions of the various terms. [b] These values are calculated at the MP2/DZP++//RHF/6-31G* level of theory.

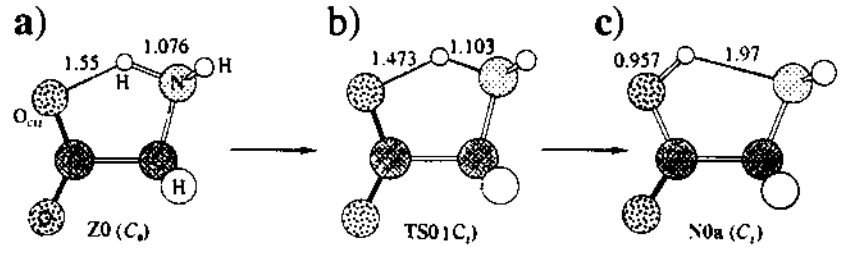

Figure 1. RHF/6-31G* optimized structures of (a) **Z0**, (b) **TS0**, and (c) **N0a**. The atom shading defined in part a is used throughout this paper.

Z0 is the only "minimum" on the zwitterionic gas phase PES, any deviation from planarity will lead to an increase in the intrinsic energy. Therefore, the intrinsic glycine energy of **Z1b** is higher than that for **Z1a** (by 1.4 kcal/mol, see Table 3). The total energy of **Z1b** relative to **Z1a** of 1.3 kcal/mol can then be attributed to the higher intrinsic glycine energy of **Z1b** (Table 3).

Since **Z1a** and **Z1b** are essentially identical structures only the lower energy structure **Z1a** is considered as a starting point for proton transfer to form a neutral minimum.

2. Intramolecular Proton Transfer Transition State. The most direct path to a neutral structure is the intramolecular transfer of the proton in the intramolecular hydrogen bond. A RHF/DZP transition state (**TS1a**) for such a reaction is shown in Figure 3c. The monohydrated transition state is quite similar to the gas phase analog, but it occurs slightly later on the reaction path.[32] The largest structural change on going from **Z1a** to **TS1a** is the shortening of the intramolecular **OH** distance by 0.59 Å, while the associated NH bond is lengthened by the comparatively smaller amount of 0.128 Å. These changes in the glycine structure effect a 0.26−0.30 Å lengthening of the two water−glycine hydrogen bonds.

At the RHF/DZP level of theory the proton transfer barrier is 1.5 kcal/mol. This occurs because the decrease in the binding energy in the transition state (5.3 kcal/mol) is larger than the decrease in the intrinsic glycine energy (3.7 kcal/mol), relative to **Z1a**. However, the inclusion of electron correlation (MP2/DZP++ single point energies) lowers ΔE[Gly#] to −7.3 kcal/mol and leaves the change in binding energy essentially unchanged (see Table 3). Therefore there is no barrier at the correlated level. A similar energy analysis of the entire IRC, leading from **Z1a** to the neutral structure **N1a** (discussed in Section IIIC4) via **TS1a**, is shown in Figure 2b. This shows that the energy lowering from the internal proton transfer in glycine dominates the energy increase due to the weakening of the water−glycine hydrogen bonds throughout the reaction. Therefore it appears that **Z1a** is not a true minimum.

As an additional check, the RHF/DZP structure was used as an initial guess for a MP2/DZP geometry optimization for which the N−H bond was constrained to its RHF value. The resulting partially optimized MP2/DZP structure was then fully optimized in a second step by removing the N−H distance constraint. This full optimization led to a neutral glycine structure.

It thus appears that the zwitterionic form is not a minimum on the monohydrated glycine PES.

3. Water-Assisted Proton Transfer Transition State. Water-assisted proton transfer presents an alternative, indirect, path for the formation of a monohydrated neutral glycine. While it was established in the previous section that **Z1a** is a minimum on the Hartree−Fock surface due to the lack of electron correlation in the structure optimization, the study of water-assisted proton transfer initiated from this structure provides valuable information about the intrinsic mechanism. This analysis then serves as a reference point for more extensively hydrated systems in analogy to **TS0**.

The RHF/DZP transition state for the water-assisted proton transfer from **Z1a** (**TS1b**) is shown in Figure 3d. The breaking N−H bond is 0.168 Å longer than in **Z1a** (0.036 Å longer than in **TS1a**), while the breaking water **O**−H bond is longer in **TS1b** relative to **Z1a** by 0.197 Å. The water molecule is pulled toward glycine, to make the two forming **OH** bonds 1.219 and 1.285 Å. In the process, the intramolecular hydrogen bond is broken [the N(H)···O bond length is stretched by 1 Å].

With the inclusion of correlation **TS1b** is 3.6 kcal/mol above **Z1a**. However, the IRC initiated from **TS1b** (Figure 2c) shows

(32) Hammond, G. S. *J. Am. Chem. Soc.* **1955**, *77*, 334.

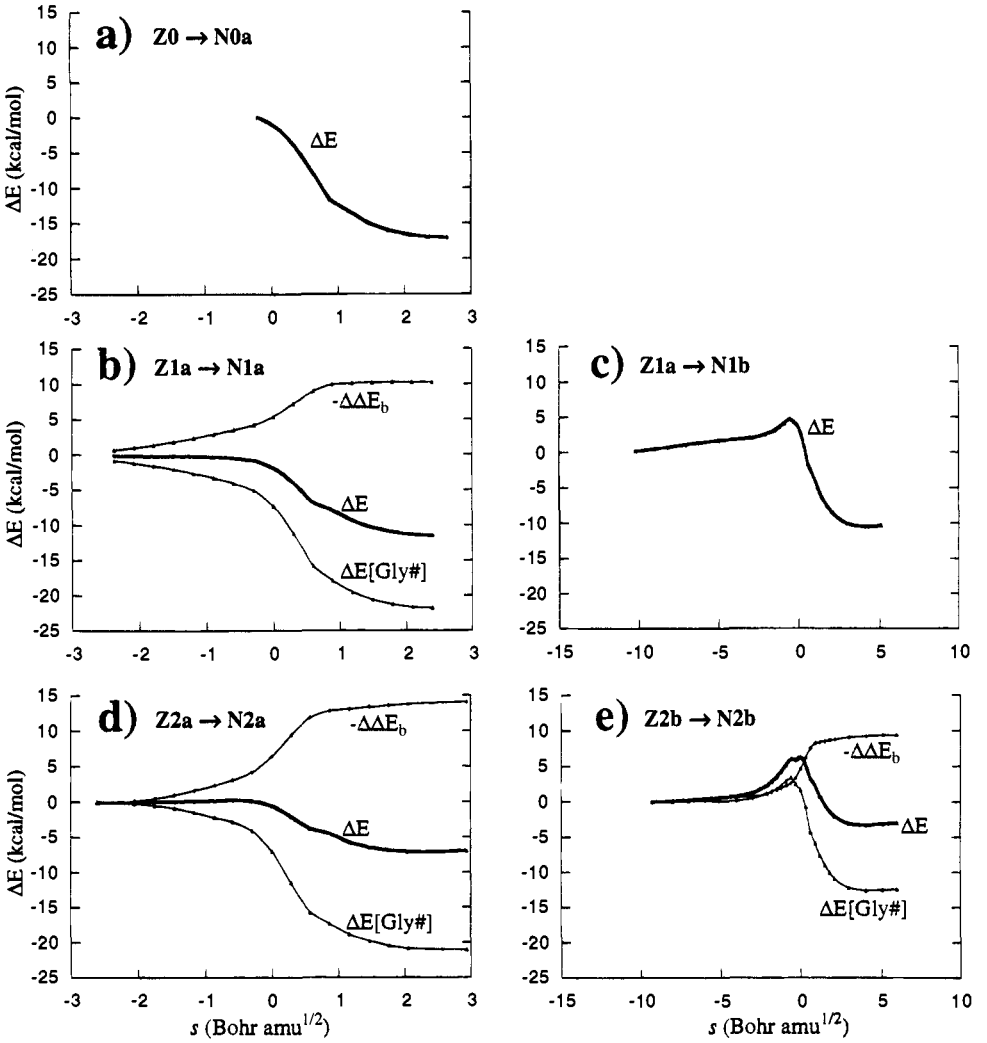

Figure 2. Plot of the total energy and its intrinsic and binding energy components (eq 8) for various IRCs. The level of theory is MP2/DZP++//RHF/6-31G* for part a and MP2/DZP++//RHF/DZP for parts b–e.

that at this correlated level the energy maximum occurs slightly before **TS1b** resulting in a 4.8-kcal/mol "barrier". The inclusion of vibrational and temperature effects lowers the energy difference by 3.4–4.6 kcal/mol, which makes **TS1b** roughly isoenergetic with **Z1a**.

4. Neutral PES. The two proton transfer paths discussed in the previous two sections lead to two different neutral minima on the monohydrated PES of glycine. The intramolecular proton transfer IRC shown in Figure 2b leads to the neutral structure **N1a** shown in Figure 3e. The two glycine–water hydrogen bonds in **Z1a** have lengthened by more than 0.5 Å. However, the binding energy has only decreased by 10.0 kcal/mol relative to the zwitterion (see Table 3), from 18.3 kcal/mol to 8.3 kcal/mol. The glycine structure itself retains the intramolecular hydrogen bond but the bond length is increased by 0.11 Å relative to the zwitterion. The proton transfer decreases the intrinsic glycine energy by 21.7 kcal/mol. Combined with the 10 kcal/mol loss of water binding energy this leads to an overall exothermicity of 11.8 kcal/mol. The addition of vibrational effects increases the exothermicity further by 1–2 kcal/mol (see Table 3).

The water-assisted proton transfer IRC shown in Figure 2c leads to the neutral structure **N1b** shown in Figure 3f. Judging from the interatomic distances, this structure has strong intermolecular hydrogen bonds, especially between the water and the COOH group. Consequently the binding energy has only decreased by 6.7 kcal/mol upon proton transfer. The glycine structure **N1b** has no intramolecular hydrogen bond, and the heavy atom framework deviates from planarity by 44.4° (Table 2). The intrinsic energy is 3.6 kcal/mol higher than for **N1a**, but since the binding energy is larger for **N1b**, the overall exothermicity for **Z1a** → **N1b** is 10.4 kcal/mol, only slightly less than that for **Z1a** → **N1a**.

In a previous study of the PES of monohydrated neutral glycine, Stevens and Basch[15] identified five stationary points with C_s symmetry. These five structures were re-optimized without symmetry constraints at the RHF/DZP level of theory for comparison with **N1a** and **N1b**. The structures (**N1c–g**) are shown in Figure 4, and the relative energetics are presented in Table 4. All but one structure proved to be lower in energy than **N1a** and **N1b**. The two lowest energy conformers (**N1c** and **N1d**) both have the water molecule bound to the COOH group by about 11 kcal/mol. Structure **N1c** is lower in energy (by 1.2 kcal/mol) than **N1d** due to its lower intrinsic energy (1.6 kcal/mol). The next two structures in Figure 4 have the water molecule associated with both functional groups. Structure **N1e** has an intermolecular hydrogen bond to the nitrogen plus a weak interaction with the C=O oxygen, while **N1f** has two intermolecular hydrogen bonds: one to the C=O oxygen and another to one of the NH hydrogens. The binding energies of these two structures bracket that of **N1a** which also has a bridging water molecule. Together with the relative internal glycine energies this results in total energies for **N1e**, **N1f**, and **N1a** of 3.4–3.7 kcal/mol relative to the global minimum **N1c**.

Scheme 2. RHF/6-31G* Energies (in kcal/mol) Relative to **Z1a** and Imaginary Frequencies[a]

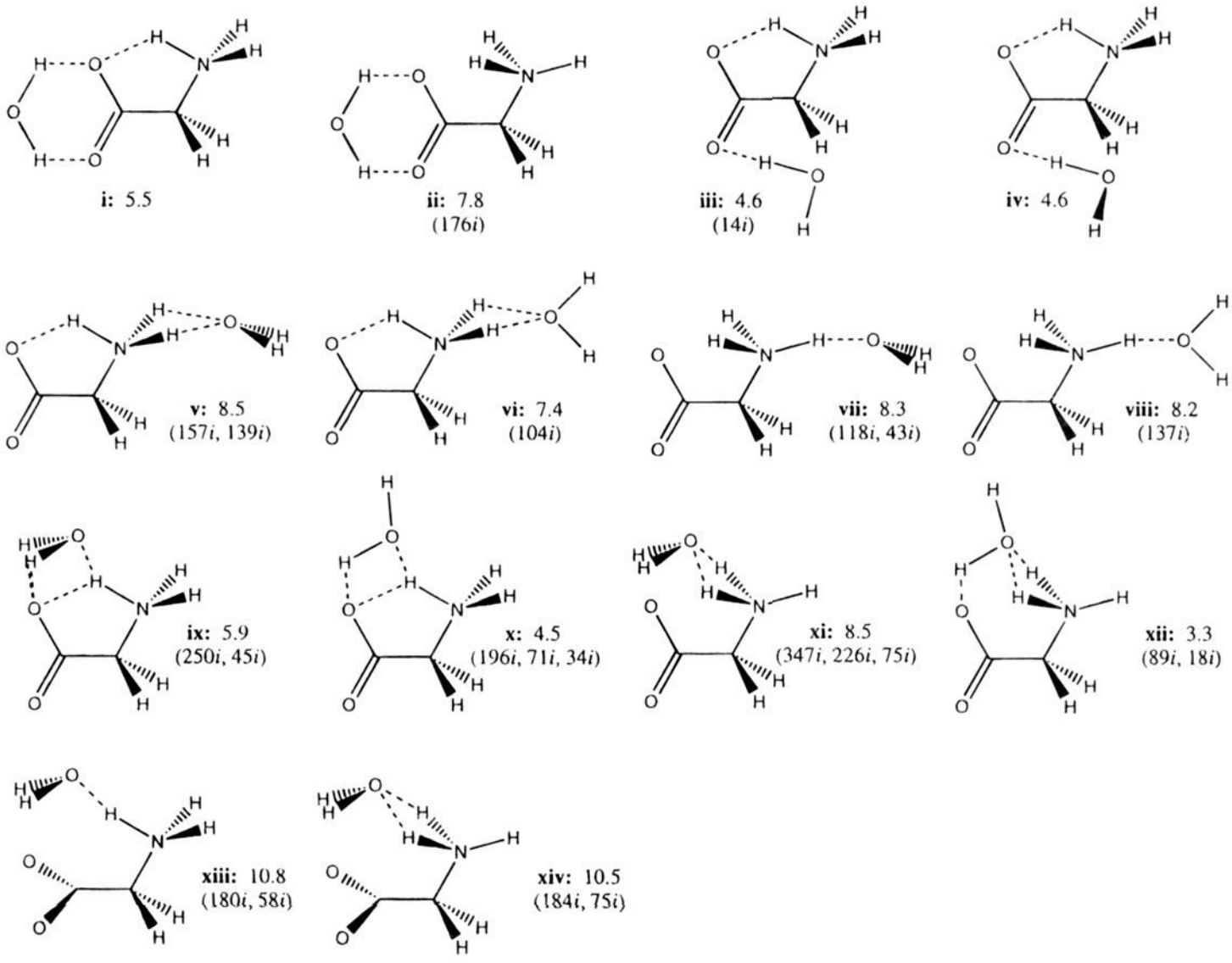

[a] All structures except **iv** were optimized within C_s symmetry.

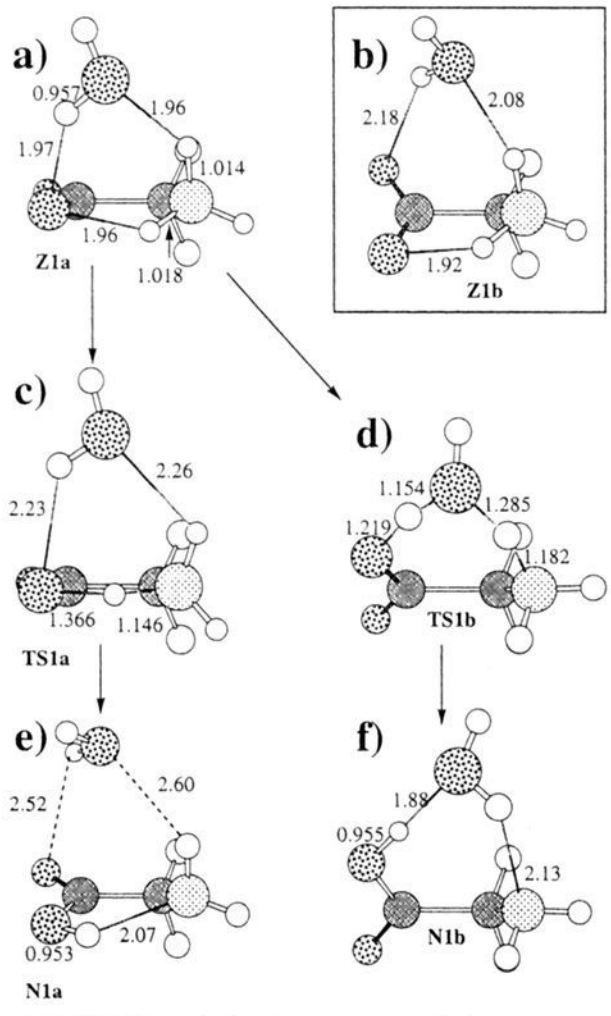

Figure 3. RHF/DZP optimized structures of the two monohydrated zwitterionic structures and the transition states and neutral minima resulting from proton transfer. Bond lengths are in Å.

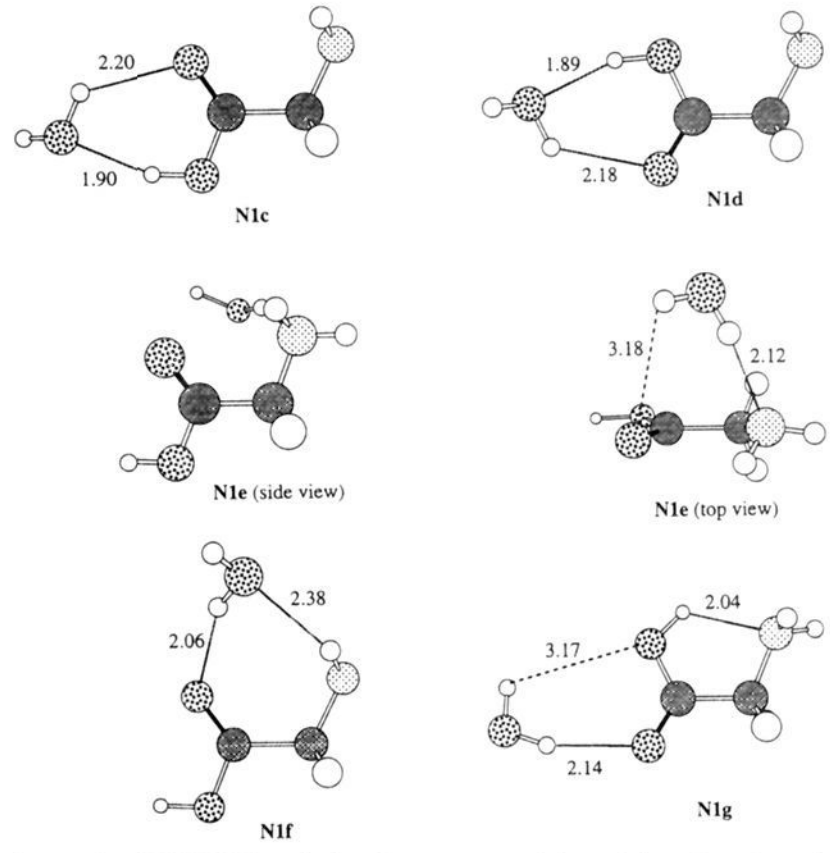

Figure 4. RHF/DZP optimized structures of the minima found on the neutral monohydrated glycine PES. Bond lengths are in Å.

Structure **N1g** has the water molecule bound to the C=O oxygen by 6.3 kcal/mol. This is the weakest binding energy of all the monohydrated glycine structures considered here. The glycine structure resembles **N0a** and the difference in intrinsic energy thus contributes 1 kcal/mol to the total relative energy of 5.4 kcal/mol. Structure **N1b** has the largest binding energy of the neutral glycine structures on the monohydrated PES (11.7 kcal/mol). However, the internal geometry, which resembles **N0a**, lacks the intramolecular hydrogen bond and the intrinsic glycine energy is large (5.8 kcal/mol) as a result. This leads to a high net relative energy of 5.6 kcal/mol.

D. Glycine(H_2O)$_2$. 1. Zwitterion PES. The most promising candidates for minima on the dihydrated zwitterionic surface

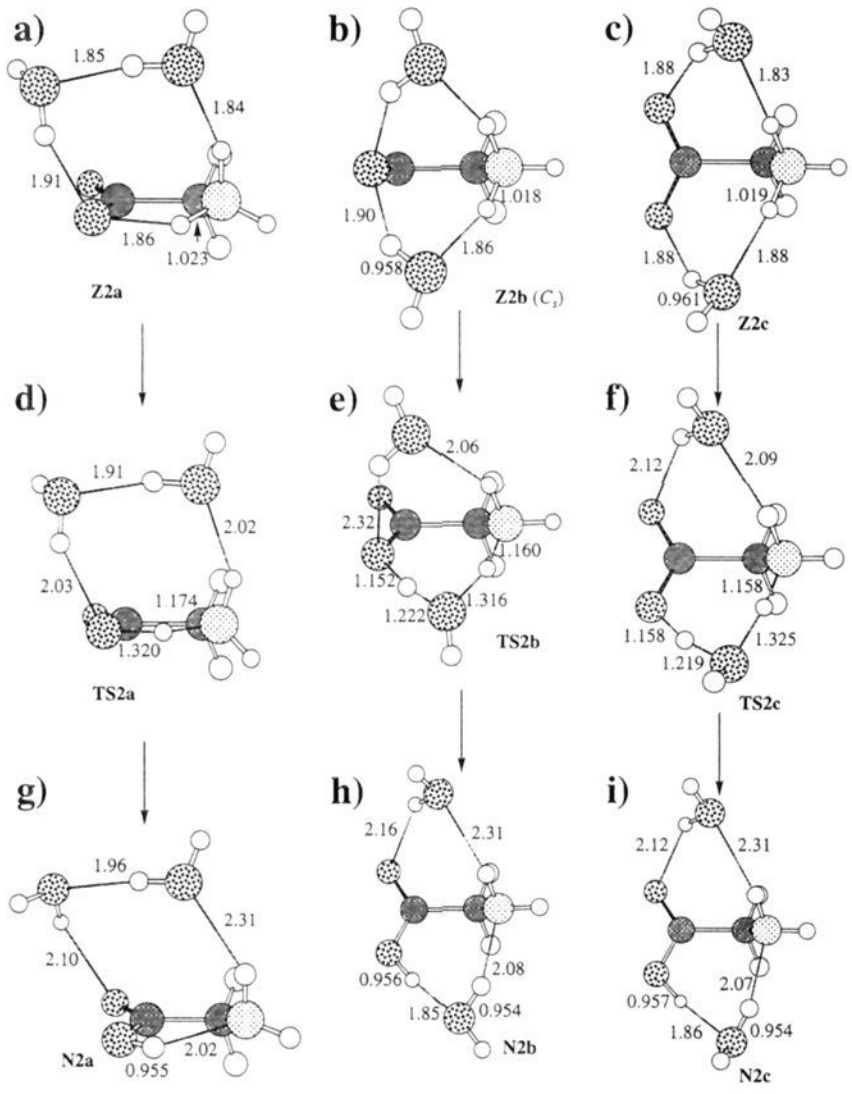

Figure 5. RHF/DZP optimized structures of the three dihydrated zwitterionic structures (a−c) and the transition states (d−f) and neutral minima (g−i) resulting from proton transfer. Bond lengths are in Å.

were chosen based on the results in the previous section. Two such candidates, which combine the water−glycine arrangements of **Z1a** with **i** and **iv** from Scheme 2, are shown here.

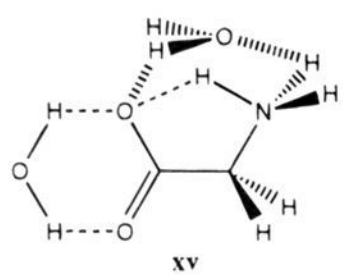

xv

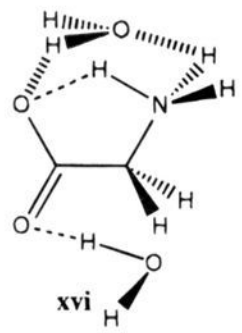

xvi

A complete geometry optimization of structure **xv** led to **Z2a** shown in Figure 5a. A water glycine−hydrogen bond associated with each water in **xv** has been broken to form a water−water hydrogen bond in **Z2a**. Upon geometry optimization structure **xvi** is 6.1 kcal/mol higher in energy than **Z2a** ($\Delta H_0 = 5.8$ and $\Delta G_{298} = 4.9$ kcal/mol). Due to this relatively high energy **xvi** is not considered further. Another (C_s) structure, **Z2b** (Figure 5b), has both water molecules in a bridging arrangement similar to **Z1a**. A similar C_s structure in which the in-plane NH_3^+ hydrogen points toward the COO^- group is a transition state to rotation about the CN bond in **Z2b**. A third structure, **Z2c** (Figure 5c), has a similar bridging arrangement of the water molecules except that they are hydrogen bonded to different oxygens in the COO^- group, which is perpendicular to the NH_3^+ group. The geometry of **Z2c** is slightly distorted from C_s symmetry since the C_s structure has a small ($23i$ cm^{-1}) imaginary frequency with an associated a″ normal mode.

The relative energetics for **Z2a−c** are presented in Table 4. The three structures are within 1.3 kcal/mol in total relative energy (the inclusion of vibrational and temperature effects increases that value by 1.1 kcal/mol): **Z2a** is the lowest, followed by **Z2b** which is 0.7 kcal/mol higher. The overall relative energies follow the same trend as the intrinsic glycine energies, although the energy range of the latter spans 11 kcal/mol! Thus, *just two water molecules can introduce a significant distortion of the structure of glycine without a large increase in overall energy*. This is because the distortion of the glycine molecule affords a stronger interaction with the two water molecules as is evidenced by the binding energies (Table 4). Structures **Z2b** and **Z2c** have binding energies that are 4.3 and 9.6 kcal/mol larger than that of **Z2a**.

Since structures **Z2a−c** are fairly close in energy and quite different in structure, all three were selected as starting points for proton transfer to form neutral structures.

2. Intramolecular Proton Transfer Transition State. Of the three structures, **Z2a−c**, only **Z2a** has an intramolecular hydrogen bond and can transfer a proton intramolecularly. The transition state for such a reaction (**TS2a**) is shown in Figure 5d. The glycine geometry is similar to **TS1a**: the intramolecular OH distance is shorter by 0.54 Å, while the associated NH bond is longer by 0.151 Å, so **TS2a** is a slightly later[32] transition state than **TS1a**. The lengthenings of the water−glycine hydrogen bonds relative to **Z2a** are only 0.12−0.18 Å, less than half that for **TS1a** relative to **Z1a**.

The RHF/DZP barrier is 2.8 kcal/mol, but the inclusion of electron correlation (MP2/DZP++ single point energies) makes the transition state energy 0.6 kcal/mol lower than the energy of the zwitterion (Table 3). Just as for **TS1a**, electron correlation lowers the relative intrinsic glycine energy from −3.5 to −7.0 kcal/mol while the change in binding energy is well described by RHF/DZP ($\Delta\Delta E_b = -6.3$ and −6.4 kcal/mol for RHF/DZP and MP2/DZP++, respectively). Figure 2d shows that when MP2/DZP++ electron correlation is added, the intrinsic glycine energy decrease is larger in magnitude than the decrease in the binding energy along the entire RHF/DZP IRC. In addition, vibrational effects decrease the transition state energy further, by 3 kcal/mol, relative to the zwitterion. Thus, **Z2a** does not appear to be a true minimum.

3. Water-Assisted Proton Transfer Transition States. Neither **Z2b** or **Z2c** have an intramolecular hydrogen bond, so proton transfer must be assisted by one of the water molecules. Transition states for the water-assisted proton transfer initiated from **Z2b** and **Z2c** (**TS2b** and **TS2c**) are shown in Figure 5e and 5f, respectively. The two transition states are very similar since their heavy atom frameworks have similar deviations from planarity (32.7−58.4°, Table 2). The covalent bonds that are broken or formed are within 0.01 Å of one another in the two transition states. The breaking N−H bond is 0.03 Å shorter, but the breaking O−H bond is 0.07 Å longer, in both **TS2b** and **TS2c** compared to **TS1b** and so it is not possible to say that the latter transition state is later or earlier than the two former transition states. The water−glycine hydrogen bonds are elongated (by 0.20−0.42 Å) for both **TS2b** and **TS2c** relative to their respective minima.

The two barriers associated with **TS2b** and **TS2c** as well as their binding and intrinsic energy components are listed in Table 3. In order to use the glycine(H_2O) results as a reference, the intrinsic energy is taken to be that of the glycine−water complex corresponding to the **Z1a** → **N1b** water-assisted reaction discussed previously, and the binding energy is that of the other, "spectator", water molecule. The relative intrinsic energies of both transition states **TS2b** and **TS2c** are lower than the 3.6 kcal/mol classical barrier height for **Z1a** → **N1b**; in fact the intrinsic energy of **TS2c** is lower (by 1.3 kcal/mol) than that of **Z2c**. The overall barriers of 6.3 and 4.4 kcal/mol are mainly due to the 4.7- and 5.6-kcal/mol decrease in the binding energy

for **TS2b** and **TS2c** relative to **Z2b** and **Z2c**, respectively. The relative contributions of $\Delta\Delta E_b$ and ΔE[Gly#] to the total relative energy along the entire IRC connecting **Z2b** with **N2b** are shown in Figure 2e. Figure 2e reveals that the relative intrinsic energy reaches a maximum shortly before $s = 0$, just as for **Z1a** → **N1b** (Figure 2c), after which it falls below the decrease in interaction energy. The interaction energy changes most rapidly around the RHF transition state region, and as a result the MP2/DZP++ and RHF/DZP energy maxima coincide (the latter occurs at $s = 0$ by definition). The inclusion of vibrational effects lowers the electronic barrier heights by 4−5 kcal/mol, so that the free energy barrier for **Z2b** → **N2b** is 1.9 kcal/mol at 298 K. *Structure* **Z2b** *thus appears to be a true zwitterionic minimum.* Structure **Z2c** does not appear to be a stable minimum when vibrational effects are added (see ΔH_0 in Table 3), but there is an entropic stabilization (ΔG_{298}) that provides a very slight net stability for this species.

4. Neutral PES. The three proton transfer paths discussed in the previous two subsections lead to three different neutral minima on the dihydrated PES of glycine. The intramolecular proton transfer IRC shown in Figure 2d leads to neutral structure **N2a** shown in Figure 5g. The intermolecular hydrogen bond distances have increased by 0.11−0.47 Å relative to the zwitterion and the binding energy has decreased by 13.1 kcal/mol as a result. The change in the intrinsic energy of glycine is −20.7 kcal/mol, very similar to the monohydrated value of −21.7 kcal/mol. The overall exothermicity is therefore 7.6 kcal/mol, and it is increased by 1.3 kcal/mol upon inclusion of vibrational effects.

The two water-assisted proton transfer reactions lead to nearly identical neutral minima, **N2b** and **N2c** (Figure 5h and 5i). The intrinsic glycine−water energy difference of **N2b** and **N2c**, relative to **Z2b** and **Z2c**, is −12.3 and −16.3 kcal/mol, respectively (Table 3). The latter is larger in magnitude mainly because the intrinsic energy of **Z2c** is 3.0 kcal/mol higher than that of **Z2b**. Both are larger than the energy of **N1b** relative to **Z1a** because the intrinsic energies of both **Z2b** and **Z2c** are higher than that of **Z1a**. The total relative energy of **N2b** of −3.8 kcal/mol makes **Z2b** → **N2b** the least exothermic reaction considered in this study. Vibrational effects increase the exothermicity to 5−6 kcal/mol. The reaction **Z2c** → **N2c** has an overall exothermicity of 5.5, 6.7, and 7.3 kcal/mol for ΔE, ΔH_0, and ΔG_{298}, respectively.

Since the global energy minimum on the dihydrated PES clearly will be a neutral structure the neutral region of the surface was explored further, and the results are shown in Figure 6 and Table 4. Just as for the neutral monohydrated PES, the lowest energy conformers (**N2d** and **N2e**) are found by hydrating the COOH group. Both structures combine high binding energies and low intrinsic glycine energies which result in low total relative energies: 0.0 and 1.0 for **N2d** and **N2e**, respectively. Structure **N2a** is 3.3 kcal/mol higher in energy than **N2d**, due mostly to the lower binding energy of **N2a**. Structures **N2b** and **N2c** prove to be relatively high energy conformers on the neutral PES. The relative energy of **N2b** is 7.8 kcal/mol. This is due mainly to the relatively high intrinsic glycine energy.

5. Conformational Interconversion of Zwitterionic Structures. Since both **Z2a** and **Z2c** are apparently unstable with respect to proton transfer, the conformational conversion of **Z2b** to **Z2a** or **Z2c** may represent alternative paths for proton transfer from **Z2b** that are energetically more favorable. In order to address this question the conformational transition states for **Z2b** ↔ **Z2a** (**TS2d**) and **Z2b** ↔ **Z2c** (**TS2e**) were located and verified by calculating the pertinent IRCs. These two transition states are presented in Figure 7, together with their energies

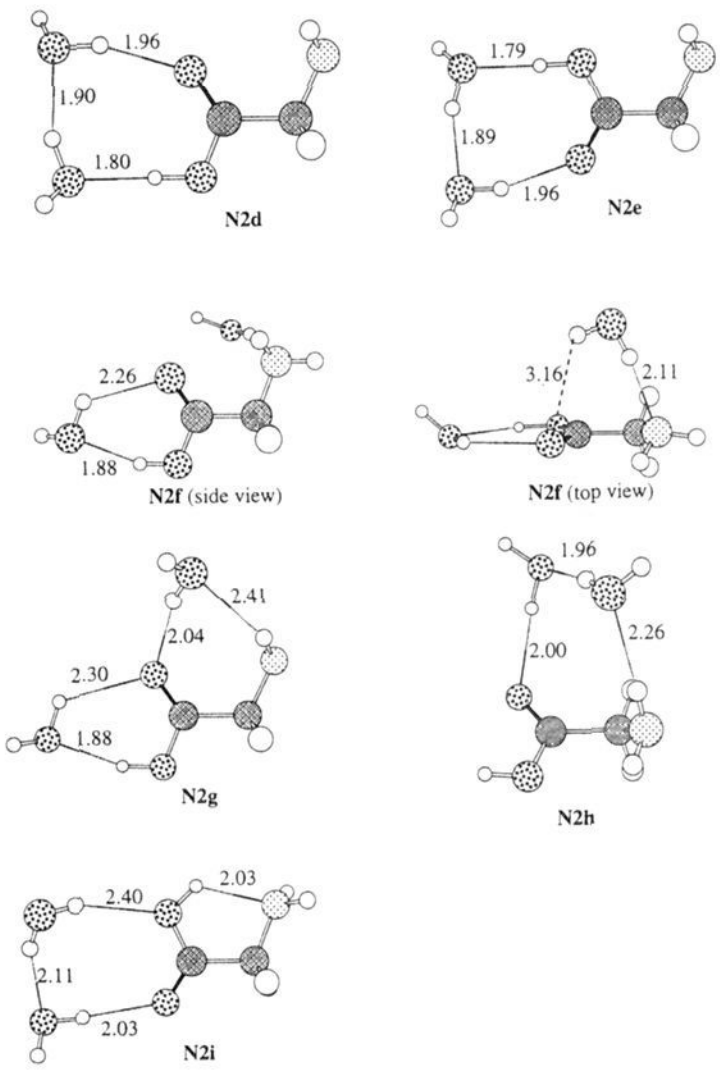

Figure 6. RHF/DZP optimized structures of the minima found on the neutral dihydrated glycine PES. Bond lengths are in Å.

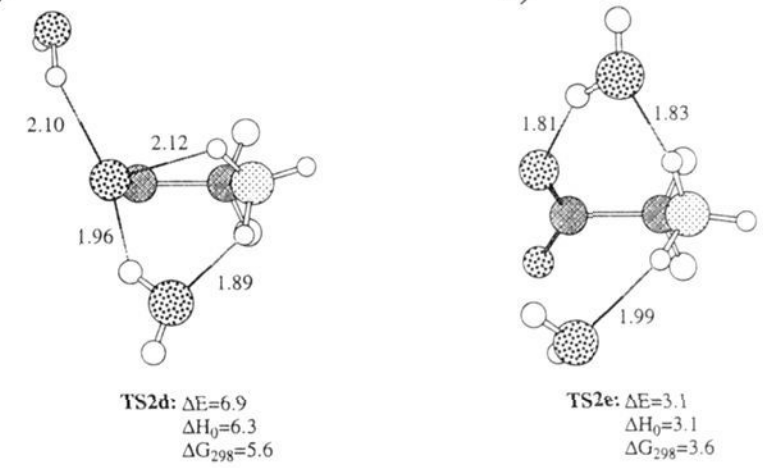

Figure 7. RHF/DZP optimized structures of the transition states connecting **Z2b** with (a) **Z2a** and (b) **Z2c** and the barrier heights relative to **Z2b**. Bond lengths are in Å and energies are in kcal/mol.

relative to **Z2b**. On the electronic energy surface the energy requirement for proton transfer in **Z2b** (6.3 kcal/mol) is comparable to that for isomerization to **Z2a** (6.9 kcal/mol) and about twice as large as that for isomerization to **Z2c** (3.1 kcal/mol). However, once vibrational and temperature effects are included the proton transfer barrier (1.9 kcal/mol) is lower than the barriers to conformational interconversion 5.6 and 3.6 kcal/mol for isomerization to **Z2a** and **Z2c**, respectively.

IV. Analysis

One of the goals of this study is to obtain a good understanding of mono- and dihydrated glycine based on quantum mechanics. The binding energy analysis (eq 8) of mono- and dihydrated structures shows that their energies are dominated by the intrinsic energy of glycine. Therefore, it is necessary to analyze the intrinsic energy of glycine further. Three very basic questions present themsevles immediately: (1) Why is the neutral structure lower in energy than the hypothetical zwitter-

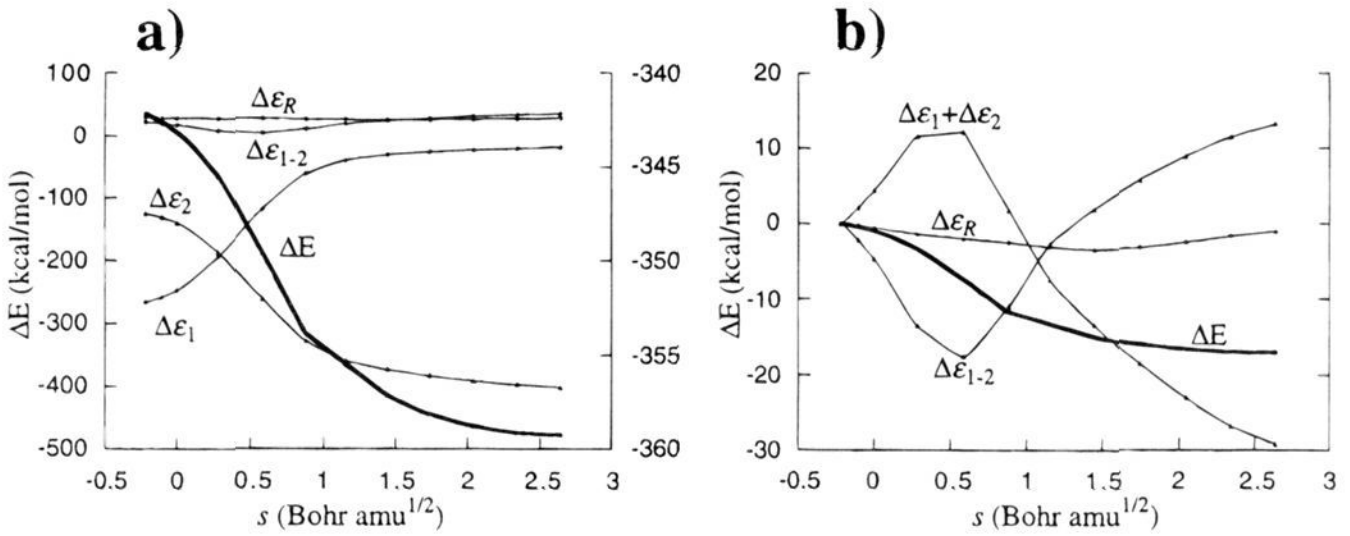

Figure 8. (a) Plot of the four energy components defined in eq 12 (left vertical axis) and the total energy (bold curve, right vertical axis), relative to their respective components in the glycine anion. (b) Plot of $\Delta\epsilon_1 + \Delta\epsilon_2$ and the remaining energy components relative to their respective values in the zwitterion. In these and subsequent plots the bold curve represents the sum of the remaining curves. Energies are evaluated at the MP2/DZP++//RHF/6-31G* level of theory.

ionic structure? (2) Why is there no barrier to proton transfer in the gas phase? (3) Why is there a barrier to water-assisted proton transfer? The theory of localized charge distributions,[26] outlined in Section II, is used to address these questions. The first two questions are considered in Section A and the third question is considered in Section B.

A. Analysis of the Gas Phase Proton Transfer IRC. 1. Nuclear Charge Partitioning. The energy localization of the glycine SCF wavefunction yields 20 localized molecular orbitals (LMOs). In order to get a continuous description of intermediate structures along the reaction path, reactants and products must be described by identical sets of LCDs. One solution is to describe all structures along the IRC as $[NH_2CH_2COO + H^+]$. To facilitate this, an additional "LCD", consisting only of a +1 charge at the position of the proton being transferred, is defined (i.e. no LMO is associated with this LCD). The 21 LCDs are divided into four "functional" groups:

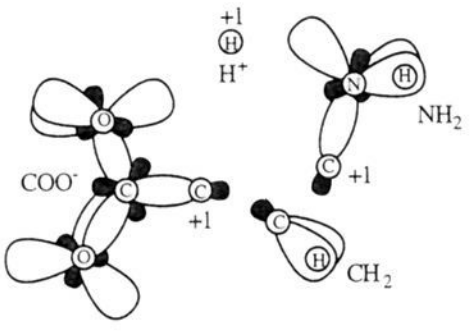

(1) One is simply the proton LCD. (2) The NH_2 group consists of the N lone pair, the two NH bonds, the N core, and the CN bond LCD. (3) The CH_2 group consists of the C core and the two CH bond LCDs. (4) The COO^- group consists of the remaining LCDs, including the CC bond LCD. The formal −1 charge on the latter group is assigned for convience to O_{cis} (the oxygen involved in the proton transfer) by assigning $+^5/_3$ to each of its three lone pair LMOs, rather than the full +2 charge prescribed by eq 1.

2. Total Energy Partitioning. The energy associated with each functional group (X) is given by,

$$E(\mathrm{X}) = \sum_{i\in \mathrm{X}}[T_i + \sum_{j\in \mathrm{X}} v_{ij} + \sum_{j\in \mathrm{X}} \mathrm{e}_{ij}^{(2)}] \qquad (9)$$

and the interaction energy between groups X and Y is

$$E(\mathrm{X}|\mathrm{Y}) = \sum_{i\in \mathrm{X}}[\sum_{j\in \mathrm{Y}}(v_{ij} + v_{ji}) + \sum_{j\in \mathrm{Y}}(\mathrm{e}_{ij}^{(2)} + \mathrm{e}_{ji}^{(2)})] \qquad (10)$$

Using these definitions the total energy can be written as

$$E = \epsilon_1 + \epsilon_2 + \epsilon_{1-2} + \epsilon_R \qquad (11)$$

where

$$\epsilon_1 = E(NH_2) + E(NH_2|H^+) = \epsilon_{NH_3^+}$$

$$\epsilon_2 = E(COO^-) + E(COO^-|H^+) = \epsilon_{COOH}$$

$$\epsilon_{1-2} = E(NH_2|COO^-) = \epsilon_{int} \qquad (12)$$

$$\epsilon_R = E(CH_2) + E(CH_2|H^+) + E(CH_2|NH_2) + E(CH_2|COO^-) = \epsilon_{CH_2}$$

3. Origin of the Z0 → N0a Exothermicity. Figure 8 shows the four energy components in eq 12 (left vertical axis) along the IRC, relative to their respective values for the glycine anion $NH_2CH_2COO^-$. So, ΔE at the zwitterion structure corresponds to the affinity for a proton at the nitrogen, while ΔE at the neutral end of the IRC corresponds to the proton affinity at the oxygen. The difference in these two proton affinities, is, of course, the energy difference between the zwitterionic and neutral structures (17 kcal/mol). The net ΔE may be analyzed in terms of the four components as follows: $\Delta\epsilon_1$ evaluated at the zwitterion structure represents the proton affinity of the NH_2 group in the zwitterion, while $\Delta\epsilon_2$ evaluated at the neutral structure represents the proton affinity of the COO^- group in the neutral species or the negative of the COOH gas phase acidity. The difference between these two quantities (135 kcal/mol) is very similar to the analogous difference between CH_3NH_2 and CH_3COO^- (129 kcal/mol) and represents the strong preference of the proton for the oxygen end of the molecule. *This difference in proton affinities of the two functional groups in glycine is the reason that the neutral structure is lower in energy than the zwitterionic structure.*[33] This 135-kcal/mol preference is reduced to the net neutral−zwitterionic ΔE of 17 kcal/mol primarily due to the values of $\Delta\epsilon_1$ at the neutral structure (−19 kcal/mol) compared with $\Delta\epsilon_2$ at the zwitterionic structure (−125 kcal/mol). These favor the zwitterion by a net 106 kcal/mol, but this is insufficient to overcome the relative proton affinities discussed above.

(33) A similar argument, which inspired this discussion, can be found in ref 4.

(34) (a) Hillenbrand, E. A.; Scheiner, S. *J. Am. Chem. Soc.* **1984**, *106*, 6266. (b) Scheiner, S. *Acc. Chem. Res.* **1989**, *18*, 174.

(35) Pritchard, R. H.; Kern, C. W. *J. Am. Chem. Soc.* **1969**, *91*, 1631.

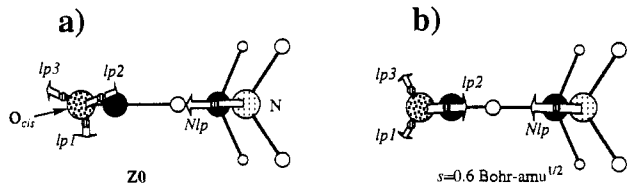

Figure 9. (a) Structure **Z0** (top view) on which the location of the centroids (small circles) of electronic charge of the N and O_{cis} lone pairs are shown. The arrows centered on these centroids represent LCD dipoles. (b) Same as for part a but for the structure at $s = 0.6$ bohr-amu$^{1/2}$.

4. Why There Is No Barrier. The two energies, $\Delta\epsilon_1$ and $\Delta\epsilon_2$ taken along the entire IRC (Figure 2a), represent the proton dissociation potentials used by, e.g., Scheiner[34] to analyze proton transfer reactions. Following ref 34b, the proton transfer between NH_2 and COO^- is decomposed into two separable but simultaneous processes: the dissociation of the proton from NH_2 (represented by $\Delta\epsilon_1$ in Figure 8a) and its association with COO^- ($\Delta\epsilon_2$). The sum of these two potentials is then a first approximation to the total energy of the proton transfer. Figure 8b shows this approximate total energy, together with the two remaining energy components and the true total energy ΔE, all relative to their respective values for the zwitterion. It is clear from this figure that $\Delta\epsilon_1 + \Delta\epsilon_2$ is not a good approximation to the total energy in this case, since this sum has a 10-kcal/mol barrier to proton transfer. This "barrier" is more than cancelled by a concomitant 18-kcal/mol "minimum" in the interaction energy $\Delta\epsilon_{1-2}$. Thus within the framework of the energy partitioning outlined above, *the lack of a barrier to proton transfer is due to an initial decrease in the interaction energy between the NH_2 and COO^- groups as the proton is transferred.* Careful examination of the individual energy components reveals that the single largest contributor to this initial decrease is the interaction between the lone pair LCD on N and one of the lone pairs on the oxygen involved in proton transfer (O_{cis}). A *qualitative* explanation in terms of LCD charge and dipolar interactions, obtained at the RHF/DZP++ level of theory, follows.

Figures 9a and 9b show the position of the centroids of electronic charge of the N (*Nlp*) and O_{cis} lone pair LMOs (*lp1-3*) for the zwitterion and the structure at $s = 0.6$ bohr-amu$^{1/2}$ (where $\Delta\epsilon_{1-2}$ is a minimum), respectively. The arrows represent the dipole moments due to the LCD charge distributions[26c-h,35] evaluated at each centroid. A close look at the LMOs indicates that in the zwitterionic structure the O_{cis} lone pairs are in an arrangement that is intermediate between that of a CO single bond, with three similar lone pairs, and that of a CO double bond with two lone pairs and two CO "banana" bonds. On going to the $s = 0.6$ structure, where the O_{cis} lone pairs are in an arrangement corresponding to a CO single bond, the interaction of the N lone pair LCD and *lp1* on O_{cis} changes from slightly repulsive to attractive. The resulting decrease in the interaction energy of these two lone pairs is largely responsible for the initial decrease of $\Delta\epsilon_{1-2}$ as the proton is transferred. For interpretive purposes the interaction of the N and three O_{cis} lone pairs may be approximated by a charge dipole plus a dipole–dipole interaction (the net $-1/3$ charge for each of the O_{cis} LCDs is placed at their centroids). Such an analysis of the *Nlp–lp1* interaction energy ascribes the interaction energy lowering to a less repulsive charge–dipole and more attractive dipole–dipole interaction on going from **Z0** to the latter structure.

B. Analysis of the Water-Assisted Proton Transfer IRC.

1. Partitioning of the Nuclear Charge and Total Energy. The structures along the IRC (Figure 2c) are described in terms of $[NH_2CH_2COO^- + OH^- + H_1^+ + H_2^+]$, where H_1^+ and H_2^+ are transferred to and from the OH^- group, respectively. The glycine anion is divided into three functional groups as described above, so there is a total of six functional groups. The formal minus charge of the OH^- group is assigned to the O atom as before by assigning a $+5/3$ charge to each of the three O lone pairs.

The total energy is decomposed into a contribution from the proton transfer from the NH_2 group to the OH^- group (ϵ_I) and the OH^- group to the COO^- group (ϵ_{II}). There is also an interaction energy ϵ_{I-II}, and all contributions from the methylene group, ϵ_R:

$$E = \epsilon_I + \epsilon_{II} + \epsilon_{I-II} + \epsilon_R \tag{13}$$

Both ϵ_I and ϵ_{II} are composed of a term due to proton dissociation, association, and an interaction term,

$$\epsilon_I = \epsilon_1 + \epsilon_2 + \epsilon_{1-2} \quad \text{and} \quad \epsilon_{II} = \epsilon_3 + \epsilon_4 + \epsilon_{3-4} \tag{14}$$

where

$$\epsilon_1 = E(NH_2) + E(NH_2|H_1^+) = \epsilon_{NH_3^+}$$

$$\epsilon_2 = {}^1/_2E(OH^-) + E(OH^-|H_1^+) = \epsilon_{H_2O_A}$$

$$\epsilon_{1-2} = E(NH_2|OH^-)$$

$$\epsilon_3 = E(COO^-) + E(COO^-|H_2^+) = \epsilon_{COOH}$$

$$\epsilon_4 = {}^1/_2E(OH^-) + E(OH^-|H_2^+) = \epsilon_{H_2O_B}$$

$$\epsilon_{3-4} = E(COO^-|OH^-) \tag{15}$$

Only one-half of the OH^- energy is included in ϵ_2 and ϵ_4 to avoid double counting it. The last two energy terms are given by

$$\epsilon_{I-II} = E(H_1^+|H_2^+) + E(NH_2|COO^-) + E(NH_2|H_2^+) + E(COO^-|H_1^+)$$

$$\epsilon_R = E(CH_2) + \sum_{Y \neq CH_2} E(CH_2|Y) = \epsilon_{CH_2} \tag{16}$$

2. Origin of the Barrier. Figure 10a shows a plot of $\Delta\epsilon_I + \Delta\epsilon_{II}$, $\Delta\epsilon_{I-II}$, and $\Delta\epsilon_R$, evaluated relative to their values in the zwitterion, along the water-assisted proton transfer IRC shown in Figure 2c (see Figure 8c for comparison). It is evident from Figure 10a that within this energy partitioning scheme *the electronic energy barrier is due to* $\Delta\epsilon_{I-II}$. The combined energy from the two simultaneous proton transfer reactions, $\Delta\epsilon_I + \Delta\epsilon_{II}$, is dominated by $\Delta\epsilon_I$ since H_1^+ is being transferred between the two groups with the largest difference in proton affinity (NH_2 and OH^-). When the proton is transferred from NH_2 to OH^-, $\Delta\epsilon_I$ is always decreasing. Figure 10b shows a breakdown of $\Delta\epsilon_{I-II}$ into its four components (eq 16). Clearly, the two most important contributions to $\Delta\epsilon_{I-II}$ are the interactions between the two protons and between the NH_2 and COO^- groups. The former energy is simply a reflection of the change in proton–proton distance during the reaction, while the behavior of the latter energy can be *qualitatively* explained in terms of (RHF/DZP++) LCD net charges and dipoles, as explained below. Figures 11a and 11b show the location of the LMO centroids and the associated LCD dipoles of the N and O_{cis} lone pairs for **Z1a** and **TS1b**, respectively. The large increase in $E(NH_2|COO^-)$ is mainly a result of the increase in the interaction energy of *lp1* and *lp2* with *Nlp*. On going from **Z1a** to **TS1b** there is a small clockwise rotation about the CN bond and as a result the *Nlp* and *lp1* and *lp2* changes from attractive to repulsive. In addition there is a small counterclockwise rotation about the

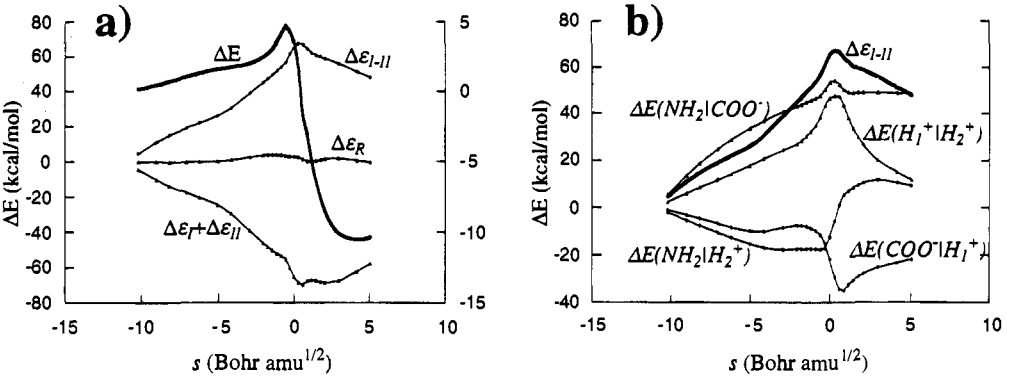

Figure 10. (a) Plot of $\Delta\epsilon_I + \Delta\epsilon_{II}$ and the remaining energy components in eq 13 (left vertical axis) and the total energy (bold curve, right vertical axis) relative to their respective values in the zwitterion. (b) Plot of $\Delta\epsilon_{I-II}$ and its components (eq 16) relative to their respective values in the zwitterion.

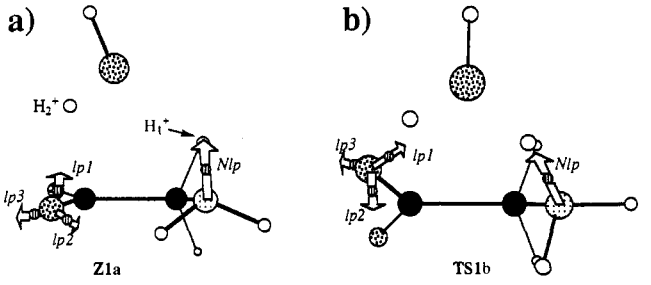

Figure 11. (a) Structure **Z1a** (top view) on which the locations of the centroids of electronic charge of the N and O_{cis} lone pairs are shown. The arrows centered on these centroids represent LCD dipoles. (b) Same as for part a but for **TS1b**.

C−O bond which makes the *Nlp−lp1* and *Nlp−lp2* dipole−dipole interactions more repulsive and less attractive, respectively. The charge dipole and dipole−dipole energy terms make roughly equal contributions to the energy increase.

V. Summary

The effect of solvation by one or two water molecules on mechanisms for proton transfer in the glycine zwitterion is considered in this study. *It is found that two water molecules stabilize the glycine zwitterion*, so that it appears to be a minimum on the potential energy, adiabatic ground state, and 298 K free energy surfaces. In particular:

(1) One and two water molecules are not sufficient to stabilize zwitterionic structures for which direct intramolecular proton transfer is possible, i.e. structures that contain intramolecular hydrogen bonds. This is because of the decrease in the interaction energy between the COO^- and NH_2 groups during the initial stage of proton transfer.

(2) Two water molecules give rise to structures with and without intramolecular hydrogen bonds that are essentially isoenergetic.

(3) Structures without intramolecular hydrogen bonds can transfer the proton via a water molecule, and for one such structure (**Z2b**) the free energy barrier is 1.9 kcal/mol. This structure is kinetically stable with respect not only to proton transfer but also to conformational conversion to other dihydrated zwitterionic structures. It therefore may be observable at low temperatures.

(4) The water-assisted proton transfer mechanism is energetically more demanding because of the increase in the interaction energy between the COO^- and NH_2 groups, and between the two transferring protons, during the initial stage of proton transfer.

(5) The lowest energy conformers on both the mono- and dihydrated PES are neutral structures with the water molecule(s) bound to the COOH group (**N1c** and **N2d**, respectively). These structures combine relatively strong binding energies with low intrinsic glycine energies. The latter can be attributed to the high proton affinity of the COO^- group relative to the NH_2 group.

(6) Structure **N2d** is 11.6 kcal/mol lower in energy than **Z2b**.

The barrier to proton transfer in dihydrated glycine appears to be at most a few kilocalories per mole. This suggests that the level of theory necessary to *unequivocally* state whether a dihydrated zwitterion structure may be observed experimentally will remain prohibitively expensive for some time. However, our results suggest that an experimental investigation is warranted.

Acknowledgment. The authors are indebted to Drs. Walter Stevens, Brian Wladkowski, and Michael Schmidt as well as Mr. Simon Webb for helpful discussions. Mr. Brett Bode's assistance in preparing Figures 9 and 11 is gratefully acknowledged. J.H.J. acknowledges an ISU College of Letters, Arts, and Sciences Research Assistantship. This work was supported in part by grants from the National Science Foundation (CHE-9317317) and the Air Force Office of Science Research (92-0226). The calculations reported here were performed on IBM RS6000 workstations generously provided by Iowa State University and on the 16 node iPSC/860 Paragon at the Air Force Phillips Laboratory.

JA9509902